This article has been accepted for publication in a future issue of this journal, but has not been fully edited. Content may change prior to final publication. Citation information: DOI 10.1109/TIV.2017.2788186, IEEE Transactions on Intelligent Vehicles

$\mathcal{L}_1$ Adaptive Control of Vehicle Lateral Dynamics

Mehran M. Shirazi, Graduate Student Member, *IEEE*, Ahmad B. Rad, *Senior Member, IEEE*

***Abstract*— In this paper, we present an application of $\mathcal{L}_1$ adaptive control for the vehicle lateral control problem. The main objective is to design a controller that ensures the vehicle follows the reference trajectory (center of the lane) with robustness to uncertain parameters of the vehicle lateral dynamics. The designed $\mathcal{L}_1$ adaptive control signal compensates the uncertainties and variations in model parameters in the presence of disturbances. A bicycle model for vehicle lateral dynamics is considered. We will demonstrate the desirable performance of the proposed adaptive controller at steady-state as well as the transient response. The simulation results confirm that the controller significantly improves the transient response of the vehicle lateral controller in the presence of wind gusts, road bank angle, icy or slippery road conditions, and other parameter uncertainties and unknown disturbances.**

***Index Terms*— $\mathcal{L}_1$ Adaptive Control, Autonomous Vehicles, Lateral Control, Robust Control**

I. Introduction

VEHICLE lateral control is an integral part of autonomous and intelligent vehicle control systems. The primary goal of the lateral control, also referred to as steering control, is to navigate a car along the desired path (lane keeping/following). In addition, performing lane change maneuvers, avoiding obstacles and collisions in emergency situations are also directly related to vehicle lateral control.

Data from Federal Highway Administration (FHWA) suggests that crashes caused by lane deviation account for about 53 percent of all fatal crashes [1]. More than half a million road accidents are due to improper lane changing executions [2] which makes it one of the dangerous driving acts in highways. In emergency obstacle avoidance cases, less experienced drivers have difficulty in performing evasive maneuvers and stabilizing the vehicle after the maneuver. Advanced Driver Assistance Systems are expected to alleviate the number of these three types of accidents by assisting the drivers in lane-keeping, lane changing, and emergency collision avoidance tasks. Also, driverless cars also need to have high-performance steering control systems.

The vehicle lateral controller should be able to maintain the car in the center of the lane in the presence of disturbances and uncertainties. In addition, the parameters of the vehicle dynamics are not constant and depend on the car speed, weather, road, and tire conditions. Therefore, the system should be able to follow the reference road trajectory by compensating the effects of all uncertainties, noises, disturbances, and parameter variations.

As lateral control is central to driving, it has been extensively studied. [3, 4]. Among the methodologies employed are linear quadratic control (LQ) [5], lead-lag control [6], optimal preview control [7], sliding mode control [8], virtual curvature method for lane change [9], extended Kalman filter [10], and genetic algorithm [11]. Some researchers have tried to imitate human steering behavior using fuzzy logic controllers [12], artificial neural networks [13], and also by using the neuromuscular dynamics [14].

In the last decade, following the implementation and excellent performance of model predictive controllers (MPC) in various industrial projects [15], many researchers and companies in automotive industries have started using this algorithm for the lateral control of autonomous vehicles. For example, MPC was used for double change maneuver in [16]. Lee and Yoo designed a controller using MPC algorithm using sideslip angle and vehicle velocity [17]. In 2010, Anderson et al. applied MPC to plan optimal vehicle trajectories to keep the vehicle in a safe corridor [18].

The above selective literature review shows the significance and importance of lateral control in autonomous vehicles. However, the problem presents additional challenges when external disturbances, uncertainties, and parameter variations are considered. These complexities are less considered in the literature. Therefore, it is envisaged that robust adaptive control is an excellent candidate to address these problems successfully.

Less than a decade ago, $\mathcal{L}_1$ adaptive control was introduced by Hovakimyan and Cao [19-21]. The following properties of this controller make it a suitable choice for the vehicle lateral control problem. The key features of this control architecture are guaranteed robustness and fast adaptation. These ensure that the control system is robust to variations in the uncertainty and parameters of the system as well as demonstrating an acceptable performance. The $\mathcal{L}_1$ control algorithm also ensures uniformly bounded transient response and steady-state tracking. This is achieved by proper formulation of the control objective in a way that the uncertainties of the system can be compensated for within the bandwidth of the control channel [19]. In this algorithm, the decoupling of adaptation and robustness is made possible by building the robustness specifications in the problem formulation. This increases the speed of adaptation

Footnote!

.

This article has been accepted for publication in a future issue of this journal, but has not been fully edited. Content may change prior to final publication. Citation information: DOI 10.1109/TIV.2017.2788186, IEEE Transactions on Intelligent Vehicles

which will be restricted only by hardware limitations. In other words, employing $\mathcal{L}_1$ adaptive control addresses fast adaptation which is beneficial for both robustness and performance. One of the crucial steps in this algorithm is selecting the underlying filter structure. This can be addressed using classical and robust control techniques.

The first and most notable application of $\mathcal{L}_1$ adaptive control was in flight control for aircraft, missiles, and spacecraft [22-25]. These flight tests included different sources of un-modeled dynamics and unknown and variable parameters. Current flight tests are being performed on a prototype commercial jet at NASA. Other than Unmanned Aerial Vehicles (UAV), this algorithm has also been used successfully in drilling systems [26], anesthesia delivery [27], wind turbines [28], and some other industrial systems [19].

Within the above context, the contribution of this communication is two folds: (i) The algorithm will guarantee stability and performance in trajectory (lane center) tracking in the presence of model uncertainties, wind disturbance, road banking angle, and icy roads, assuming there is no sensor failure. (ii) The proposed controller will rapidly adapt to variations in the parameters of the system model and compensate the effects of unknown disturbances. Also, since this method is adaptive, it is a suitable choice for vehicle lateral control problem in the presence of parameter variations. Lastly, because of its guaranteed robustness, $\mathcal{L}_1$ adaptive controller is an appropriate controller for handling vehicle lateral model uncertainties and disturbances such as the wind, slippery roads, and road banking angles.

This paper is organized as follows. The vehicle lateral dynamics model, used for the controller design and simulations, are described in Section II. In Section III, the L_1 adaptive controller theory is presented. Controller design and simulation results are described and analyzed in Section IV. Finally, conclusions are presented in Section V.

II. Vehicle Lateral Dynamics

A. Nominal Model

A nonlinear six-degree-of-freedom (DOF) vehicle model, which represents the vehicle lateral dynamics as realistically as possible, is developed in [29]. This complex model has sixteen state variables: twelve for the six DOF motions (three translational and three rotational) and four for the tires. A simplified linear two-degree of freedom 'bicycle' model of the vehicle can be obtained from the complex model. Several studies have already established that the simplified model, which we will use in this work, is a good approximation of the complex model for all practical purposes [16, 29, 30]. In this model, the vehicle yaw angle ψ and lateral position y are considered as the two degrees of freedom of the car, as shown in Fig. 1. We consider O as the center of the rotation of the vehicle. The lateral position of the car can be measured along the y axis to the point O. The yaw angle is considered as the angle between horizontal axis of the car (x) and the global horizontal axis (X). This is demonstrated in Fig. 1.

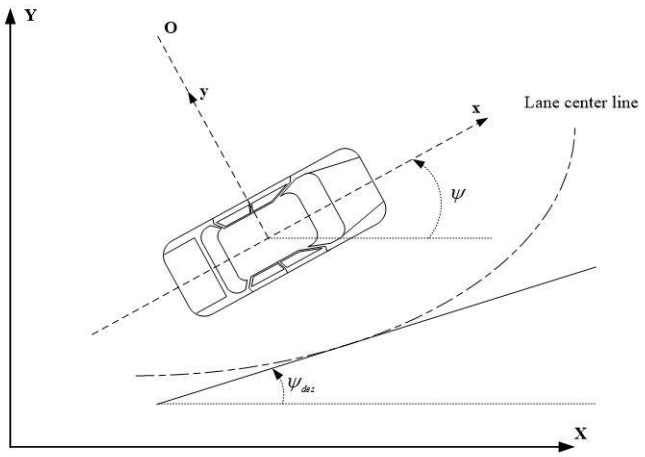

Fig. 1. Lateral vehicle dynamics

The longitudinal velocity of the car at its center of gravity is denoted by V_x. The distances of the front and rear tires from the center of gravity and cornering stiffness of each front and rear tire are shown by l_f, l_r, C_{af} and C_{ar}, respectively. The steering angle is shown by δ and the yaw moment of inertia of the vehicle is I_z. Considering lateral position, yaw angle, and their derivatives as the state variables, and using Newton's second law for motion along the y-axis, the state-space model of lateral vehicle dynamics can be shown by the following equation [30]:

$$\frac{d}{dt}\begin{bmatrix} y \\ \dot{y} \\ \psi \\ \dot{\psi} \end{bmatrix} = \begin{bmatrix} 0 & 1 & 0 & 0 \\ 0 & -\frac{2C_{af}+2\,C_{ar}}{mV_x} & 0 & -V_x - \frac{2C_{af}l_f - 2\,C_{ar}l_r}{mV_x} \\ 0 & 0 & 0 & 1 \\ 0 & -\frac{2C_{af}l_f - 2\,C_{ar}l_r}{I_z V_x} & 0 & -\frac{2C_{af}{l_f}^2 + 2\,C_{ar}{l_r}^2}{I_z V_x} \end{bmatrix} \begin{bmatrix} y \\ \dot{y} \\ \psi \\ \dot{\psi} \end{bmatrix} + \begin{bmatrix} 0 \\ \frac{2C_{af}}{m} \\ 0 \\ \frac{2C_{af}l_f}{I_z} \end{bmatrix} \delta \quad (1)$$

The ultimate goal in this paper will be designing a lateral control (steering control) for the lane keeping in autonomous vehicles. Therefore, we prefer to convert the above state-space representation of lateral dynamics to a model where the state variables are the position and orientation errors with respect to the center of the lane [31]. Therefore, the above lateral model can be re-defined in terms of two error variables: e_1 which is the distance of the center of the gravity of the vehicle from the center line of the lane and e_2 which is the orientation error of the vehicle with respect to the road.

Assuming the radius of the road is R, the rate of change of the desired orientation of the vehicle can be defined as

$$\dot{\psi}_{des} = \frac{V_x}{R} \quad (2)$$

Based on the above state variables, the tracking objective of the lateral control problem can be expressed as a problem of stabilizing the following dynamics at the origin:

This article has been accepted for publication in a future issue of this journal, but has not been fully edited. Content may change prior to final publication. Citation information: DOI 10.1109/TIV.2017.2788186, IEEE Transactions on Intelligent Vehicles

$$\frac{d}{dt}\begin{bmatrix} e_1 \\ \dot{e}_1 \\ e_2 \\ \dot{e}_2 \end{bmatrix} = \begin{bmatrix} 0 & 1 & 0 & 0 \\ 0 & -\frac{2C_{af}+2C_{ar}}{mV_x} & \frac{2C_{af}+2C_{ar}}{m} & -\frac{2C_{af}l_f-2C_{ar}l_r}{mV_x} \\ 0 & 0 & 0 & 1 \\ 0 & -\frac{2C_{af}l_f-2C_{ar}l_r}{I_zV_x} & \frac{2C_{af}l_f-2C_{ar}l_r}{I_z} & -\frac{2C_{af}{l_f}^2+2C_{ar}{l_r}^2}{I_zV_x} \end{bmatrix} \begin{bmatrix} e_1 \\ \dot{e}_1 \\ e_2 \\ \dot{e}_2 \end{bmatrix} + \begin{bmatrix} 0 \\ \frac{2C_{af}}{m} \\ 0 \\ \frac{2C_{af}l_f}{I_z} \end{bmatrix} \delta + \begin{bmatrix} 0 \\ -V_x - \frac{2C_{af}l_f-2C_{ar}l_r}{mV_x} \\ 0 \\ -\frac{2C_{af}{l_f}^2+2C_{ar}{l_r}^2}{I_zV_x} \end{bmatrix} \dot{\psi}_{des} \quad (3)$$

The lateral position of the vehicle with respect to the road is usually measured at a location ahead of the vehicle, as shown in Fig. 2. Various sensors have been used by researchers to measure this lateral error [32].

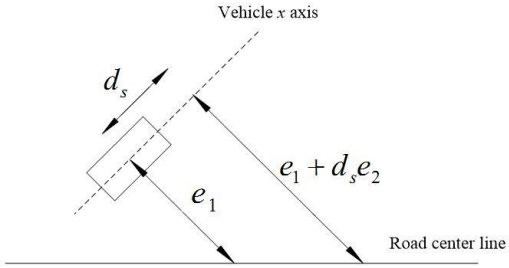

Fig. 2. Measurement of the lateral position of the vehicle

Assuming that e_2 is small, we can approximate the chord length by arc length. Therefore, the output equation of the state-space, the equation that expresses the output as a linear combination of the states, is as follows:

$$y = e_1 + d_s e_2 \quad (4)$$

where d_s is the look-ahead distance, which is the longitudinal distance of the point ahead of the vehicle center of gravity, where we make the sensor measurements.

B. Road Bank Angle

The bank angle is the angle at which the vehicle is inclined about its longitudinal axis with respect to the horizontal. Road bank angle has a direct influence on the vehicle dynamics. Whereas quantities like speed or lateral error can be obtained by direct measurement, bank angle cannot be measured as easily. Although some methods for estimating this value have been reported [33], the decoupling of parametric uncertainties (such as variations of cornering stiffness of tires and vehicle mass) from the road bank angle still needs to be addressed.

Compensating the road bank angle is neglected in many of the lateral control algorithms. In this work, we treat this variable as a disturbance or an unknown input to the vehicle and include it in all closed-loop simulations. We expect the control algorithm to compensate its effect without having any measurement of its value. The effect of the road bank angle is considered in the dynamic model of the vehicle by adding the following term to the right-hand side of (3):

$$\begin{bmatrix} 0 \\ g \\ 0 \\ 0 \end{bmatrix} \sin(\phi) \quad (5)$$

where g is the gravitational acceleration and ϕ is road bank angle.

C. Parametric Uncertainties

Variations of the parameters in (3) affect the vehicle dynamics. Whereas the parameters l_f, l_r, and d_s are fixed and known, mass (m), moment of inertia (I_z), longitudinal speed (V_x), and cornering stiffness (C_{af} and C_{ar}) might deviate from their nominal values.

Peng and Tomizuka showed in [29] that the most significant variations of vehicle dynamics are caused by the uncertainties in the value of cornering stiffness. The values of C_{af} and C_{ar} are affected by many factors: tire slip ratio, tire slip angle, tire pressure, load, velocity, temperature, and, most importantly, the road condition. Not only these values vary in a wide range, but also, they change the behavior of the vehicle drastically. The nominal and range of variations of the parameters are adopted from Peng and Tomizuka and tabulated in Table I [29].

TABLE I
SYSTEM PARAMETERS OF THE VEHICLE MODEL

Parameter	Symbol	Unit	Nominal	Min (relative)	Max (relative)
Mass	m	kg	1573	0.85	1.15
Moment of Inertia	I_z	$kg.m^2$	2873	0.85	1.15
Cornering Stiffness	C_{af}, C_{ar}	N/rad	80000	0.2	2

In this study, we assume all the above parametric uncertainties exist concurrently. Specifically, we assume one section of the road is icy, and the cornering stiffness drops to its minimum value, as it will be explained in section IV.

D. Wind Gust

The vehicle lateral control system should be able to maintain the car in the center of the lane when there is wind gust disturbance. The effect of the wind on vehicle lateral dynamics is derived in [29]. As per recommendation in [33], we add the following term to the right-hand side of (3):

$$\begin{bmatrix} 0 \\ F_w/m \\ 0 \\ T_w/I_z \end{bmatrix} \quad (6)$$

where F_w and T_w are wind force and torque acting on vehicle in lateral direction.

III. $\mathcal{L}_1$ ADAPTIVE CONTROL

This section presents an overview of $\mathcal{L}_1$ adaptive controller which was first reported by Cao and Hovakimyan [20, 21]. One of the main advantages of $\mathcal{L}_1$ controller over other adaptive

This article has been accepted for publication in a future issue of this journal, but has not been fully edited. Content may change prior to final publication. Citation information: DOI 10.1109/TIV.2017.2788186, IEEE Transactions on Intelligent Vehicles

control strategies is decoupling of the adaptation rate and the robustness. This is achieved by selecting an appropriate low-pass filter on the control signals. In all control algorithms, there is the issue of the trade-off between performance and robustness. The mentioned decoupling results in an easier solution for this trade-off problem. Although the trade-off between robustness and adaptation rate exists in this algorithm too, the techniques used in this method facilitates handling the trade-off problem.

Many variations of $\mathcal{L}_1$ adaptive controller have since been reported [19]. We employ a particular architecture of this controller that suitably addresses the lateral vehicle control with uncertainties on the parameters of the vehicle dynamics. This version of the controller employs output feedback in the presence of unknown time-varying nonlinearities [34]. The main reason for the selection of this algorithm is that it does not require explicit measurement of the states of the systems as sensors that measure such states may not be available.

This algorithm guarantees that the transient response for system's both signals, input and output, are uniformly bounded as compared to similar signals of a reference system. The bounds for the error signals between the controlled system and the reference system can be reduced by increasing the adaptation gain [19]. The details of these bounds and their relationships with the adaptation gain are given in [20] and [19].

A. *Problem Formulation*

In this methodology, the following structure is considered for the system

$$Y(s) = A(s)\big(U(s) + D(s)\big) \tag{7}$$

where $Y(s)$ is the Laplace transform of system's output $y(t)$, $U(s)$ is the Laplace transform of $u(t)$ which is the system's input, $A(s)$ is the unknown transfer function of the system, and $D(s)$ is the Laplace transform of the nonlinear time-varying disturbances and uncertainties, represented by $d(t) = f\big(t, y(t)\big)$. Two assumptions are made for the unknown f:

Assumption 1 (Lipschitz continuity): Arbitrary large constants $L > 0$ and $L_0 > 0$ exist such that the following inequalities hold uniformly:

$$\begin{cases} |f(t, y_1) - f(t, y_2)| \le L|y_1 - y_2| \\ |f(t, y)| \le L|y| + L_0 \end{cases} \tag{8}$$

Assumption 2: The rate of variation of uncertainties is uniformly bounded. In other words, there exist arbitrarily large constants $L_1 > 0$, $L_2 > 0$, and $L_3 > 0$ such that

$$\big|\dot{d}(t)\big| \le L_1|\dot{y}(t)| + L_2|y(t)| + L_3 \tag{9}$$

The control objective is to design an adaptive controller such that $y(t)$ tracks the reference $r(t)$ as a desired reference model $M(s)$:

$$M(s) = \frac{m}{s+m},\ m > 0 \tag{10}$$

B. $\mathcal{L}_1$ *Adaptive Control Structure*

Based on (7) and (10), the system can be written in terms of the reference system:

$$Y(s) = M(s)\big(U(s) + \sigma(s)\big) \tag{11}$$

where

$$\sigma(s) = \frac{\big(A(s) - M(s)\big)U(s) + A(s)D(s)}{M(s)} \tag{12}$$

The design of $\mathcal{L}_1$ adaptive controller involves designing a strictly proper filter $C(s)$ with $C(0) = 1$ which results in stable $H(s)$ where

$$H(s) = \frac{A(s)M(s)}{C(s)A(s) + \big(1 - C(s)\big)M(s)} \tag{13}$$

and the following norm condition is satisfied:

$$\|G(s)\|_{\mathcal{L}_1} L < 1 \tag{14}$$

with $G(s) = H(s)\big(1 - C(s)\big)$.

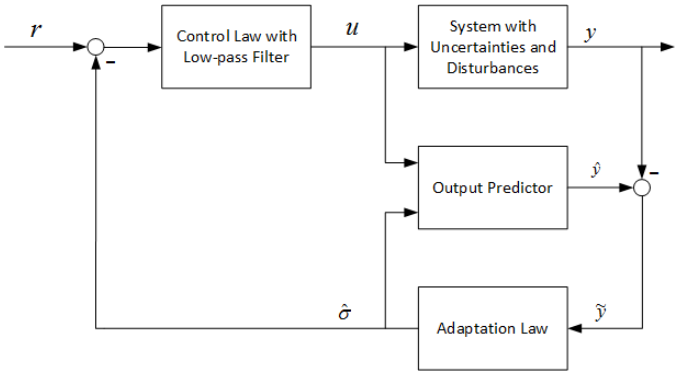

Fig. 3 Closed-loop system with $\mathcal{L}_1$ output feedback adaptive controller

The general structure of a closed-loop output feedback $\mathcal{L}_1$ adaptive controller is illustrated in Fig. 3. In addition to the control law, this algorithm consists of an output predictor and the adaptation law.

1) *Output Predictor*

The following output predictor is used here

$$\dot{\hat{y}} = -m\hat{y}(t) + m\big(u(t) + \hat{\sigma}(t)\big),\ \hat{y}(0) = 0 \tag{15}$$

where $\hat{\sigma}(t)$ is the adaptive estimate obtained by the adaptation law block.

2) *Adaptation Law*

The adaptive estimate $\hat{\sigma}(t)$ is obtained by

$$\dot{\hat{\sigma}}(t) = \Gamma\mathrm{Proj}\big(\hat{\sigma}(t), -\tilde{y}(t)\big),\ \hat{\sigma}(0) = 0 \tag{16}$$

where Proj is the projection function defined in the Appendix,

$\tilde{y}(t) = \hat{y}(t) - y(t)$ is the error between the predictor in (15) and the output of the system in (11), and $\Gamma \in \mathbb{R}^+$ is the adaptation gain. Projection is used to ensure the bounds for parameter estimation.

3) Control Law with Low-pass Filter

The following control signal is generated in this algorithm to compensate the uncertainties within the desired bandwidth:

$$U(s) = C(s)\big(R(s) - \hat{\sigma}(s)\big) \tag{17}$$

where $C(s)$ is a strictly proper low-pass filter with $C(0) = 1$. The unity dc gain of the filter ensures tracking [19]. In this work, a first-order low-pass filter is considered:

$$C(s) = \frac{\omega}{s+\omega} \tag{18}$$

C. Closed-loop Reference System

Supposing that the adaptive variable $\hat{\sigma}(t)$ is exactly estimated, $\hat{\sigma}(t) = \sigma(t)$, if we define the control signal $U(s)$ to equal $R(s) - \sigma(s)$, the output signal $Y(s)$ would exactly equal $M(s)r(s)$. However, in the $\mathcal{L}_1$ adaptive control algorithm, since we need to approximate the uncertain $\sigma(s)$ signal, the system's ideal input signal $R(s) - \sigma(s)$ is filtered with a low-pass filter $C(s)$. The main reason is to remove the high-frequency chattering phenomenon which is common in adaptive control algorithms. As a result, the expected closed-loop reference response is altered.

Assuming the uncertainties are entirely known (non-adaptive version of the adaptive controller), the closed-loop reference system would be given by

$$Y_{ref}(s) = M(s)\left(U_{ref}(s) + \sigma_{ref}(s)\right) \tag{19}$$

$$U_{ref}(s) = C(s)(R(s) - \sigma_{ref}(\mathrm{s}))) \tag{20}$$

$$\sigma_{ref}(s) = \frac{(A(s)-M(s))U_{ref}(s)+A(s)D_{ref}(s)}{M(s)} \tag{21}$$

where $D_{ref}(s)$ is the Laplace transform of $d_{ref}(t) = f\left(t, y_{ref}(t)\right)$. Substituting (21) in (20) and cancellation of $M(s)$ from both numerator and denominator, which requires a stable non-minimum phase reference model $M(s)$ to ensure stability, results in

$$U_{ref}(s) = \frac{C(s)M(s)R(s)-C(s)A(s)D(s)}{C(s)A(s)+(1-C(s))M(s)} \tag{22}$$

Substituting the closed-loop reference command (22) into (19), we get

$$Y_{ref}(s) = H(s)\left(C(s)R(s) + \big(1 - C(s)\big)D_{ref}(s)\right) \tag{23}$$

where $H(s)$ is given by (13). Therefore, $M(s)$ and $C(s)$ should be selected to ensure the stability of $H(s)$. In addition, the condition in (14) should be met so that the small-gain theorem can be applied [19].

As mentioned before, the ideal control signal would lead to the desired system response $M(s)R(s)$ by exactly cancelling all the uncertainties. Obviously, the response in the reference system in (19) and (20) is different from the ideal one. In fact, the control signal in (20) cancels only the uncertainties which are in the bandwidth of the low-pass filter $C(s)$. The parameter ω in (18) can be selected such that the bandwidth of the filter is compatible with the control channel specifications. This is exactly what one hopes to obtain in any feedback control problem in the presence of uncertainties and disturbances.

D. Designing the Controller Parameters

To design an adaptive $\mathcal{L}_1$ adaptive controller for the vehicle lateral control problem, a first-order reference model, as shown in (10), is selected. The reason is that the first-order dynamics behavior is expected from the vehicle when it is adjusting itself in the center of the lane. The parameter m in (10) should be tuned. The other parameters that need to be designed are the bandwidth (ω) of the low-pass filter in (18), and the adaptation gain (Γ) in (16).

At frequencies well below the bandwidth of the filter (way smaller than ω), the filter $C(s)$ acts similar to an all-pass filter ($C(s) \approx 1$) and from (13) we have:

$$H(s) \approx M(s) \tag{24}$$

In this case, the reference output of the system can be written using (23):

$$Y_{ref}(s) \approx M(s)R(s) \tag{25}$$

Similarly, at frequencies well above the bandwidth of the low pass filter (above ω), the filter $C(s)$ acts similar to a no-pass filter ($C(s) \approx 0$), and from (13) we have:

$$H(s) \approx A(s) \tag{26}$$

Obviously, a higher cutoff frequency (ω) in $C(s)$ results in a closed-loop reference system that acts more similarly to the desired model. However, it increases the chattering problem and reduces the stability of the system. The requirement of stability of $H(s)$ limits the range of m and ω that can be considered for designing the controller.

As mentioned, a higher ω would result in a $Y_{ref}(s)$ (response of $H(s)C(s)$) which is close to $Y_{ideal}(s)$ (response of $M(s)$). Even if these two values are close to each other, the actual closed-loop output of the system, $Y(s)$, would be different from these values if adaptation of $\sigma(s)$ is not done fast enough. In other words, the adaptation gain Γ should be selected large enough so that the output of the system follows the reference closed-loop output closely.

In summary, the control process, shown in Fig. 3, can be described as follows. The output of the unknown system, including disturbances and uncertainties, is compared to the output of the predictor in (15), which has the dynamics of the

This article has been accepted for publication in a future issue of this journal, but has not been fully edited. Content may change prior to final publication. Citation information: DOI 10.1109/TIV.2017.2788186, IEEE Transactions on Intelligent Vehicles

desired reference model. The adaptation law in (16) uses the mentioned comparison and generates the adaptive estimate $\hat{\sigma}(t)$. This adaptation estimate, in addition to the reference signal, are given to the control law with a low-pass filter in (17) to generate the control signal. The parameters which need to be tuned are m in (15), Γ in (16), and ω in (17).

The steps of the algorithm applied in this work can be summarized as follows:

1. The parameters m and ω are selected such that the condition in (13) is met. In addition, m determines the behavior of the ideal system, and ω should be large enough so that the behavior of the reference system be similar to the one of the ideal system.
2. The adaptation gain Γ is selected as large as possible such that the actual response of the system is close to the reference system. Especially, the value of Γ should not be less than the value that makes $\hat{\sigma}(t)$ unstable.
3. The prediction of the output signal ($\hat{y}(t)$) is given by (15)
4. The adaptive estimate of uncertainties ($\hat{\sigma}(t)$) is given by (16)
5. The adaptive control signal ($u(t)$) is given by (17)

IV. Simulation and Results

The dynamics of the vehicle are considered as explained in section II and parameters of this model, in the nominal case, are considered as [30]:

$$C_{af} = 80000,\ C_{ar} = 80000,\ l_f = 1.1,\ l_r = 1.58,\ I_z = 2873,\ m = 1573 \quad (27)$$

The road banking angle in (5) and the wind gusts in (6) are considered as disturbances to the system. The model parametric uncertainties in Table I and the neglected dynamics in the bicycle model are considered as the uncertainties. The look-ahead distance, where the sensor measurements are made as explained in (4), is considered $d_s = 18\ m$. One should note that in a curved road, this parameter can change accordingly.

The range of acceptable values of m and ω for stability of $H(s)$ in (13) is shown in Fig. 4. This result shows that if the reference model is selected slower than a certain speed, the cutoff frequency of the lowpass filter can be chosen arbitrarily for meeting the condition in (13).

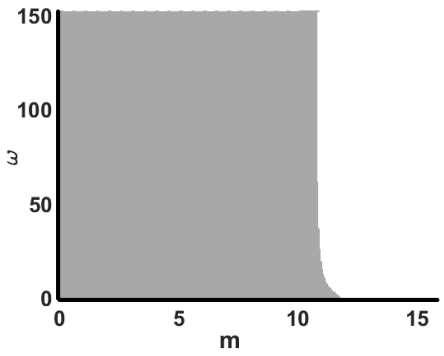

Fig. 4 Region of (m, ω) for stable $H(s)$ shown in grey

In this algorithm, the adaptive system attempts to estimate the parameter $\sigma_{ref}(t)$ by updating the parameter $\hat{\sigma}(t)$ using (16). It is proved in [35] that $\sigma_{ref}(t)$ is stable if $H(s)$ is stable. However, the controller parameters should be designed such that the signal $\hat{\sigma}(t)$ is stable too. In order to investigate the stability of this signal, we use the following equation obtained in [35]:

$$\hat{\sigma}(s) = \frac{C(s)\big(A(s)-M(s)\big)R(s)+A(s)D(s)}{\frac{1}{\Gamma}s+C(s)A(s)+\big(1-C(s)\big)M(s)} \quad (28)$$

As we expect, when $\Gamma \to \infty$, the estimate $\hat{\sigma}(s) \to \sigma_{ref}(s)$. One useful method to investigate the stability of this system, based on the variations of the adaptive gain Γ, is to use the root locus method. In order to use this method, we write the denominator of (28) as

$$1 + \Gamma T(s) \quad (29)$$

where

$$T(s) = \frac{C(s)A(s)+\big(1-C(s)\big)M(s)}{s}. \quad (30)$$

Comparing (13) and (30), we can see that the zeros of $T(s)$ match the poles of $H(s)$. Obviously if the parameters m and ω are selected in the grey area in Fig. 4, the open-loop zeros of $T(s)$, which are equal to closed-loop poles of (28) or (29) for large values of Γ, are stable. However, the poles of $T(s)$, in addition to the trivial pole at $s = 0$, match the poles $C(s)$, $M(s)$, and $A(s)$. In the vehicle lateral dynamics system, the poles of $A(s)$ are unstable even for the nominal case without uncertainties. As the adaptation gain Γ increases from 0, to ∞, the poles of $\hat{\sigma}(s)$ move from the unstable poles of $T(s)$ to the stable zeros of $T(s)$. However, the unmatched poles go to ∞ following some asymptotes. Since these asymptotes might lead to unstable right half plane, we should be specifically careful about these unmatched poles. In addition, the adaptation gain should be chosen large enough to make sure that the matched poles are stable.

We studied the effect of changing the acceptable (see Fig. 4) parameters of $C(s)$ and $M(s)$, i.e. ω and m, on the poles of $H(s)$ for the vehicle lateral dynamics (3) using nominal values mentioned in (27). If these two parameters are selected from the grey region shown in Fig. 4, the dominant real pole of $H(s)$ does not move significantly, and it is always around -0.8. However, the dominant imaginary poles strongly depend on the pair (m, ω). They would be farther from $j\omega$ axis in complex plane when m is smaller. This results in a trade-off because a smaller m is equivalent to slower response in the reference model. The root locus of (29) for the vehicle lateral dynamics for a fixed m and ω is shown in Fig. 5. The higher the parameter ω is, the higher adaptation gain Γ is required to stabilize $H(s)$. In this system, any $\Gamma > 2770$ stabilizes $\hat{\sigma}(s)$.

In all the simulations, an initial offset of 1 meter is considered for the vehicle. The wind uncertainty starts at $t = 9s$ and reaches its maximum $t = 11s$ with a force of $F_w = -500$

This article has been accepted for publication in a future issue of this journal, but has not been fully edited. Content may change prior to final publication. Citation information: DOI 10.1109/TIV.2017.2788186, IEEE Transactions on Intelligent Vehicles

Newtons and moment of $T_w = -200$ Newton-meters in the lateral direction and affects the vehicle as explained in (6). The road bank angle starts at the same time as the wind, and it affects the lateral dynamics of the vehicle in the same direction as the wind, as shown in (5). This angle reaches its maximum of 6° at $t = 11s$. The variations of both the wind and road bank angle disturbances are shown in Fig. 6. The variations of these disturbances are matched so that the behavior of the system can be studied in the worst case where the peak of both disturbances happen at the same time ($11 \leq t \leq 13$).

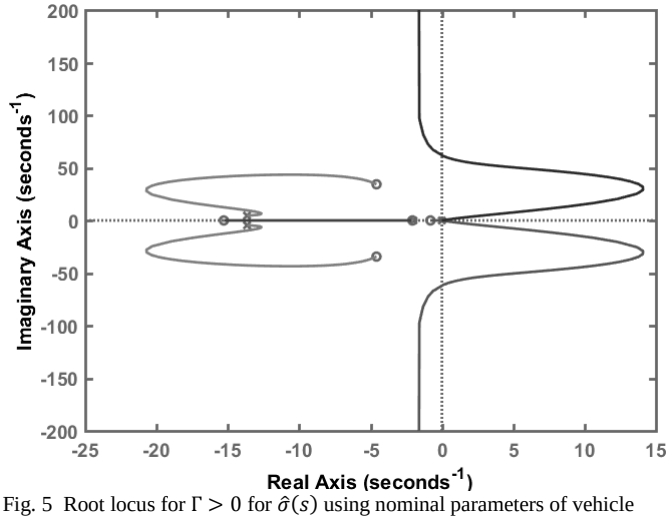

Fig. 5 Root locus for $\Gamma > 0$ for $\hat{\sigma}(s)$ using nominal parameters of vehicle lateral dynamics

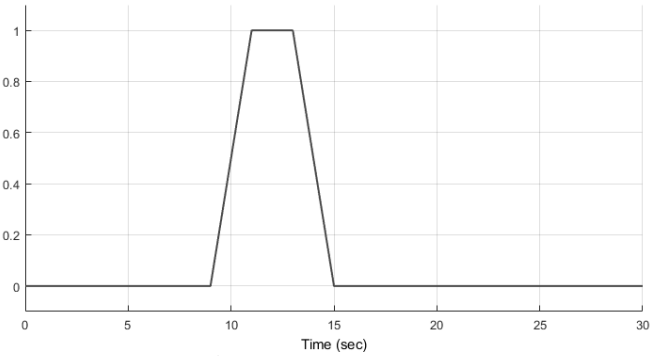

Fig. 6 Scaled variation of wind and road banking angle disturbances. The value one at $11 \leq t \leq 13$ shows the maximum value of wind force (-500N) and the maximum value of road bank angle (6°). The other values at other times are scaled accordingly between 0 and 1.

The road condition is assumed to suddenly change at $t = 11s$ to an icy section where C_{af} and C_{ar} change to 0.2 times their nominal value, as shown in Table I. The road remains icy until the end of simulations at $t = 30s$.

The performance of the $\mathcal{L}_1$ adaptive controller in steering the vehicle in the desired path, in the presence of the above uncertainties and disturbances, is compared with three other controllers. First, a conventional state feedback controller is designed to compare the performances of the controllers in the same scenario for disturbances and uncertainties. A state feedback controller that is designed for the nominal case would fail to stabilize the system in the extreme condition assumed in this scenario. Therefore, we designed the controller considering that the cornering stiffness parameters of the vehicle were at 60% of the nominal value, exactly in the middle of the nominal value and the extreme case of 20% used in the simulations. Second, a lead compensator was designed for the system. Adding phase in the gain crossover range (low-frequency range) increases the gain margin and phase margin. This results in a more robust control system in the presence of uncertainties and disturbances. Finally, a PID controller, which is known to have good disturbance rejection, is designed. The controller parameters used for all controllers in the simulations are mentioned in Table II.

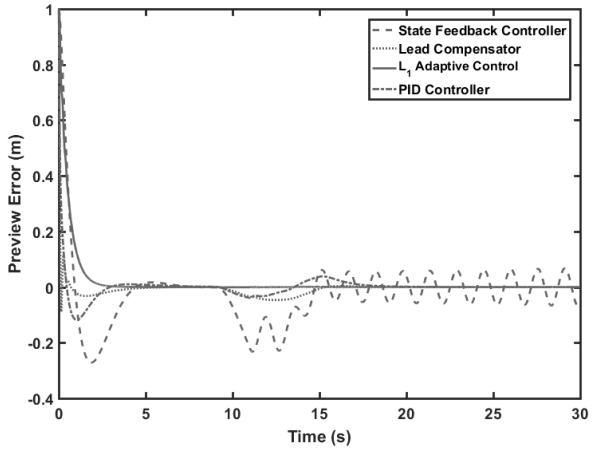

Fig. 7 Comparison of preview error of vehicle

TABLE II
THE CONTROLLER PARAMETERS USED FOR SIMULATIONS

Controller	Control Signal	Parameters
State-feedback	$u = k_1x_1 + k_2x_2 + k_3x_3 + k_4x_4$	$k_1 = 0.0137,\ k_2 = 0.0024$ $k_3 = 0.2023,\ k_4 = -0.0412$
Lead Controller	$C_L(s) = k\frac{T_ns + 1}{T_ds + 1}$	$T_n = 0.5,\quad T_d = 0.1$ $k = 0.08$
PID Controller	$C_{PID}(s) = K_P + \frac{K_I}{s} + \frac{K_DN}{1 + \frac{N}{s}}$	$K_P = 0.06,\quad K_I = 0.03$ $K_D = 0.01,\quad N = 100$
$\mathcal{L}_1$ adaptive controller	Equations (15) to (17)	$m = 2,\quad \omega = 2$ $\Gamma = 50000$

The performance of these controllers in maintaining the vehicle at the center of the lane in the presence of the above-mentioned wind gusts, road bank angle, and icy section of road is shown in Fig. 7 and Fig. 8. The outputs of the vehicle lateral system controlled by these three controllers, which equals the preview error explained in (4), are compared in Fig. 7. This figure shows that despite the sudden change in road and weather conditions, the $\mathcal{L}_1$ adaptive controller designed here can satisfactorily keep the preview error close to zero during the whole simulation time. The position of vehicle compared to the center of the lane is also shown for all controllers in Fig. 8 for $d_s = 18$. The superior performance of the controller designed here to maintain the car on the desired position can be seen in this figure. The control signals (steering wheel angles) δ generated by the controllers are demonstrated in Fig. 9. The control signal generated by all controllers are in the acceptable

This article has been accepted for publication in a future issue of this journal, but has not been fully edited. Content may change prior to final publication. Citation information: DOI 10.1109/TIV.2017.2788186, IEEE Transactions on Intelligent Vehicles

range. However, it can be seen in the zoomed section of this figure that at the beginning of the simulation, the maximum value of the steering wheel angle used by the $\mathcal{L}_1$ adaptive controller is less than a quarter of the equivalent signal generated by the lead compensator. This results in a smoother ride in the vehicle controlled by the $\mathcal{L}_1$ adaptive controller.

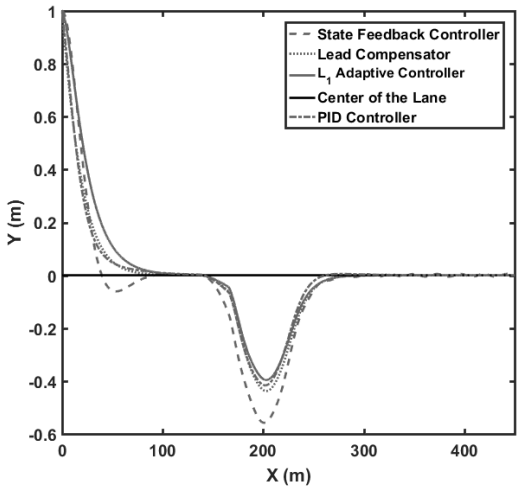

Fig. 8 Vehicle position in the presence of the wind, road banking angle, and icy section of road controlled by four different controllers

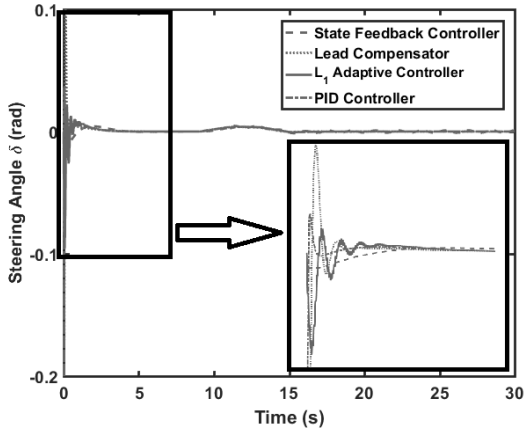

Fig. 9 Control signal (steering wheel angle) δ of the controllers

Similar simulations were performed on a curved road. The road started with straight line section, then there was a sharp left turn, and at the end, there was a long right turn, as shown in Fig. 10. The vehicle was one meter off the center of the road at the beginning of the simulations. All the extreme cases of the wind, icy road, and road banking angles explained before are included in this scenario too. As explained before, wind gusts and road banking angle end at $t = 15s$, but the icy section of the road (with 80% drop in the values of cornering stiffness) continues until the end of the simulation ($t = 30s$ and $X = 450m$). The results in Fig. 11 show the successful performance of the designed $\mathcal{L}_1$ adaptive controller in the presence of all uncertainties and disturbances. The simulation results show that the $\mathcal{L}_1$ controller maintains the vehicle at the center of the lane in all sections of the road. Results shown in Fig. 8 and Fig. 11 might suggest that the lead compensator has a faster response. However, it should be considered the $\mathcal{L}_1$ adaptive controller can maintain the vehicle at the center of the lane during the whole simulation. Based on Fig. 4, there is a limitation on the speed of the reference model (the value of m). The lateral error, e_1, for all the controllers are shown in Fig. 12. This figure confirms that the $\mathcal{L}_1$ adaptive controller has the best performance when both the disturbances and the curvy section of the road are added to the simulations. The fact that at the end of simulation the error is not zero is because that section of the road is curved (see Fig. 10) and the controller is keeping the preview error ($e_1 + d_s e_2$) at zero not the lateral error (e_1).

The steering wheel signals (δ) generated by the controllers are shown in Fig. 13. This figure shows that control signal (steering wheel) generated by $\mathcal{L}_1$ adaptive controller is in the acceptable range. Also, in the beginning of the simulation where there is a significant initial offset from the center of the lane, the lead compensator shows an aggressive behavior which does not exist in the $\mathcal{L}_1$ adaptive controller. The maximum value of the control signal in the lead controller is more than 3.5 times the maximum value of the control signal in the $\mathcal{L}_1$ adaptive controller. In the curvy section of the road, a very small amount of chattering exists in the adaptive control signal, which is negligible compared to similar adaptive controllers. The reason that the chattering is so small in this algorithm is the existence of the low-pass filter in the controller.

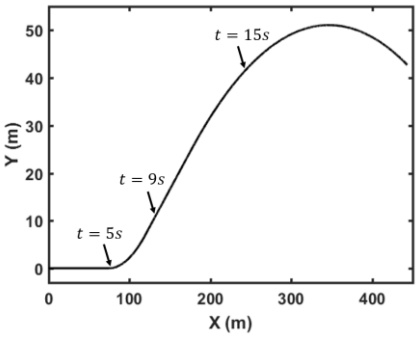

Fig. 10 Position of the center of the lane in the curved road scenario

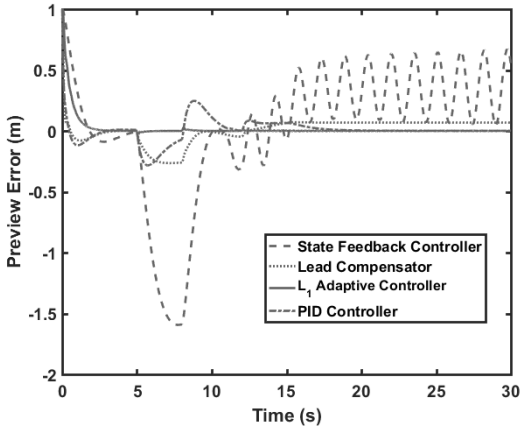

Fig. 11 Comparison of preview error of vehicle in the curved road

In order to make the simulations more realistic, measurement noise is added to the simulations and the last experiment is repeated. A normally (Gaussian) distributed random signal with zero mean and standard deviation equal to 0.05 is added to all

This article has been accepted for publication in a future issue of this journal, but has not been fully edited. Content may change prior to final publication. Citation information: DOI 10.1109/TIV.2017.2788186, IEEE Transactions on Intelligent Vehicles

the output/state measurements. Similar results to Fig. 11 are obtained (see Fig. 14). The results from the state feedback controller is not included in this figure because adding noise made the response of that controller unstable.

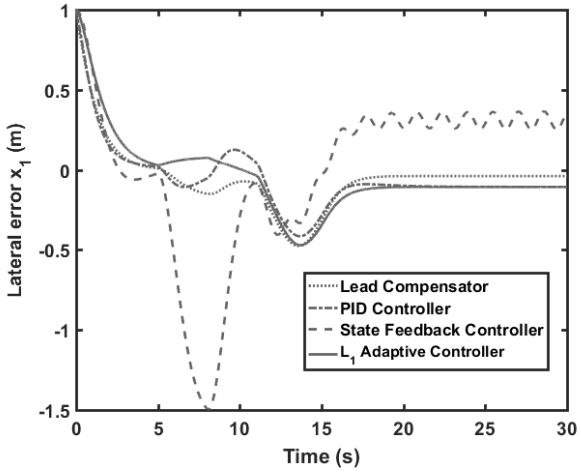

Fig. 12 Lateral error (x_1) of the vehicle in the curved road

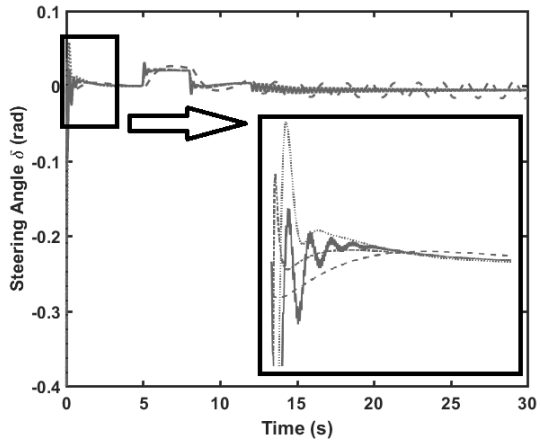

Fig. 13 Control signal (steering wheel angle) δ in the curved road

V. Conclusion

$\mathcal{L}_1$ adaptive control algorithm was utilized in this paper to design a controller for the lateral dynamics of the vehicle. Assuming the states of the system cannot be measured, an output feedback version of the algorithm was designed in this study, which makes the implementation of the controller easier. In order to test the robustness of the controller, a scenario including strong wind gusts and road banking (in the same direction of the wind) was considered. In addition, it was assumed that as soon as the wind gusts start, the road condition deteriorates and becomes icy, resulting in 80% change in the values of cornering stiffness parameters, the parameters which have the most significant effect on the vehicle dynamics.

The simulation results show that the designed lateral control algorithm has excellent robustness and disturbance rejection capability. In the challenging scenarios considered here, the conventional state feedback controller failed to keep the vehicle in the center of the lane, and the more robust lead compensator brought the lateral preview error back to zero after some deviation. However, the proposed algorithm kept error very close to zero at all simulation time, for both straight and curved roads.

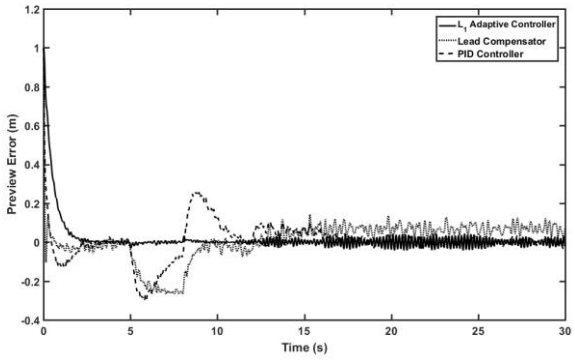

Fig. 14 Comparison of preview error when measurement noise is added

Appendix

Projection based adaptation laws in adaptive control theory are used to prevent parameter drift. The projection operator is explained in this appendix. Consider a convex set with the following smooth boundary:

$$\Omega_c \triangleq \{\theta \in \mathbb{R}^n | f(\theta) \leq c\},\ 0 \leq c \leq 1 \tag{31}$$

where $f: \mathbb{R}^n \to \mathbb{R}$ is defined as

$$f(\theta) = \frac{(\epsilon_\theta + 1)\theta^T\theta - \theta_{max}^2}{\epsilon_\theta \theta_{max}^2} \tag{32}$$

where $\epsilon_\theta > 0$ is the projection tolerance bound and θ_{max} is the norm bound we impose on θ. The definition of the projection operator follows [36]:

$$\text{Proj}(\theta, y) \triangleq \begin{cases} y & \text{if } f(\theta) < 0 \\ y & \text{if } f(\theta) \geq 0 \text{ and } \nabla f^T y \leq 0 \\ y - \frac{\nabla f}{\|\nabla f\|}\langle \frac{\nabla f}{\|\nabla f\|}, y\rangle f(\theta) & \text{if } f(\theta) \geq 0 \text{ and } \nabla f^T y > 0 \end{cases} \tag{33}$$

This means that the projection operator does not change y if θ is inside the set $\Omega_0 = \{\theta \in \mathbb{R}^n | f(\theta) \leq 0\}$. However, in $\{\theta \in \mathbb{R}^n | 0 \leq f(\theta) \leq 1\}$, if $\nabla f^T y > 0$, the projection operator subtracts a vector normal to the boundary so that a smooth transformation is obtained. In adaptive control theory, using this projection operator guarantees the boundedness of adaptive parameters, which is $\hat{\sigma}(t)$ in this work.

References

[1] FHWA, "Roadway Departure Safety," U.S. Department of Transportation 2011.

[2] D. Bevly, X. Cao, M. Gordon, G. Ozbilgin, D. Kari, B. Nelson, *et al.*, "Lane Change and Merge Maneuvers for Connected and Automated Vehicles: A Survey," *IEEE Transactions on Intelligent Vehicles*, vol. 1, pp. 105-120, 2016.

[3] A. Vahidi and A. Eskandarian, "Research advances in intelligent collision avoidance and adaptive cruise control," *Intelligent*

Transportation Systems, IEEE Transactions on, vol. 4, pp. 143-153, 2003.

[4] A. Eskandarian, *Handbook of intelligent vehicles*. London: Springer, 2012.

[5] H. Mouri and H. Furusho, "Automatic path tracking using linear quadratic control theory," in *Intelligent Transportation System, 1997. ITSC '97., IEEE Conference on*, 1997, pp. 948-953.

[6] C. Ching-Yao and T. Han-Shue, "Feasibility analysis of steering control as a driver-assistance function in collision situations," *Intelligent Transportation Systems, IEEE Transactions on*, vol. 2, pp. 1-9, 2001.

[7] H. Peng and M. Tomizuka, "Preview Control for Vehicle Lateral Guidance in Highway Automation," *Journal of Dynamic Systems, Measurement, and Control*, vol. 115, pp. 679-686, 1993.

[8] M. Canale, L. Fagiano, A. Ferrara, and C. Vecchio, "Vehicle Yaw Control via Second-Order Sliding-Mode Technique," *IEEE Transactions on Industrial Electronics*, vol. 55, pp. 3908-3916, 2008.

[9] M. L. Ho, P. T. Chan, and A. B. Rad, "Lane change algorithm for autonomous vehicles via virtual curvature method," *Journal of Advanced Transportation*, vol. 43, pp. 47-70, 2009.

[10] M. Schorn, U. Stahlin, A. Khanafer, and R. Isermann, "Nonlinear trajectory following control for automatic steering of a collision avoiding vehicle," in *American Control Conference, 2006*, 2006, p. 6 pp.

[11] M. Nagai, M. Onda, and T. Katagiri, "Simulation of emergency obstacle avoidance situations using genetic algorithm," *JSAE Review*, vol. 18, pp. 158-160, 1997.

[12] X. Wang, M. Fu, H. Ma, and Y. Yang, "Lateral control of autonomous vehicles based on fuzzy logic," *Control Engineering Practice*, vol. 34, pp. 1-17, 1// 2015.

[13] M. L. Ho, P. T. Chan, A. B. Rad, M. Shirazi, and M. Cina, "A novel fused neural network controller for lateral control of autonomous vehicles," *Applied Soft Computing*, vol. 12, pp. 3514-3525, 11// 2012.

[14] L. Bi, M. Wang, C. Wang, and Y. Liu, "Development of a Driver Lateral Control Model by Integrating Neuromuscular Dynamics Into the Queuing Network-Based Driver Model," *IEEE Transactions on Intelligent Transportation Systems*, vol. 16, pp. 2479-2486, 2015.

[15] S. J. Qin and T. A. Badgwell, "A survey of industrial model predictive control technology," *Control Engineering Practice*, vol. 11, pp. 733-764, 2003.

[16] P. Falcone, F. Borrelli, J. Asgari, H. E. Tseng, and D. Hrovat, "Predictive Active Steering Control for Autonomous Vehicle Systems," *Control Systems Technology, IEEE Transactions on*, vol. 15, pp. 566-580, 2007.

[17] J.-H. Lee and W.-S. Yoo, "An improved model-based predictive control of vehicle trajectory by using nonlinear function," *Journal of Mechanical Science and Technology*, vol. 23, pp. 918-922, 2009/04/01 2009.

[18] S. J. Anderson, S. C. Peters, T. E. Pilutti, and K. Iagnemma, "An optimal-control-based framework for trajectory planning, threat assessment, and semi-autonomous control of passenger vehicles in hazard avoidance scenarios," *International Journal of Vehicle Autonomous Systems*, vol. 8, pp. 190-216, 2010.

[19] N. Hovakimyan and C. Cao, *L1 Adaptive Control Theory: Guaranteed Robustness with Fast Adaptation* vol. 21: Siam, 2010.

[20] C. Cao and N. Hovakimyan, "Design and analysis of a novel L1 adaptive control architecture with guaranteed transient performance," *IEEE Transactions on Automatic Control*, vol. 53, 2008.

[21] C. Cao and N. Hovakimyan, "adaptive controller for systems with unknown time-varying parameters and disturbances in the presence of non-zero trajectory initialization error," *International Journal of Control*, vol. 81, pp. 1147-1161, 2008/07/01 2008.

[22] I. M. Gregory, E. Xargay, C. Cao, and N. Hovakimyan, "Flight test of L1 adaptive controller on the NASA AirSTAR flight test vehicle," in *AIAA Guidance, Navigation and Control Conference*, 2010, pp. 6.2010-8015.

[23] T. J. Leman, E. Xargay, G. Dullerud, N. Hovakimyan, and T. Wendel, "L1 adaptive control augmentation system for the X-48B aircraft," University of Illinois, 2010.

[24] J. Wang, N. Hovakimyan, and C. Cao, "L1 adaptive augmentation of gain-scheduled controller for racetrack maneuver in aerial refueling," in *AIAA Guidance, Navigation, and Control Conference*, 2009.

[25] J. Wang, C. Cao, N. Hovakimyan, R. Hindman, and D. B. Ridgely, "L1 adaptive controller for a missile longitudinal autopilot design," in *AIAA Guidance, Navigation and Control Conference*, 2008.

[26] Z. Li, N. Hovakimyan, C. Cao, and G.-O. Kaasa, "Integrated estimator and L 1 adaptive controller for well drilling systems," in *American Control Conference, 2009. ACC'09.*, 2009, pp. 1958-1963.

[27] M. A. Ralph, "L1-Adaptive Control for Anesthesia Delivery," 2011.

[28] D. Li, Y. Song, W. Cai, P. Li, and H. R. Karimi, "Wind Turbine Pitch Control and Load Mitigation Using an Adaptive Approach," *Mathematical Problems in Engineering*, vol. 2014, 2014.

[29] H. Peng and M. Tomizuka, "Lateral control of front-wheel-steering rubber-tire vehicles," *California Partners for Advanced Transit and Highways (PATH)*, 1990.

[30] R. Rajamani, *Vehicle dynamics and control*: Springer Science & Business Media, 2011.

[31] M. M. Shirazi, A. B. Rad, and O. Mohareri, "An overriding controller for vehicle lateral control system," in *ICM 2011*, 2011, pp. 128-133.

[32] C. J. Taylor, J. Kosecka, R. Blasi, and J. Malik, "A Comparative Study of Vision-Based Lateral control strategies for Autonomous highway driving," *International Journal of Robotic research*, pp. Vol. 18, No. 5, pp. 442-453, 1999.

[33] H. E. Tseng, "Dynamic estimation of road bank angle," *Vehicle System Dynamics*, vol. 36, pp. 307-328, 2001.

[34] C. Cao and N. Hovakimyan, "L1 Adaptive Output Feedback Controller for Systems of Unknown Dimension," *IEEE Transactions on Automatic Control*, vol. 53, pp. 815-821, 2008.

[35] R. Hindman, C. Cao, and N. Hovakimyan, "Designing a High Performance, Stable L1 Adaptive Output Feedback Controller," in *AIAA Guidance, Navigation and Control Conference and Exhibit*, ed: American Institute of Aeronautics and Astronautics, 2007.

[36] J. B. Pomet and L. Praly, "Adaptive nonlinear regulation: estimation from the Lyapunov equation," *IEEE Transactions on Automatic Control*, vol. 37, pp. 729-740, 1992.

Mehran M. Shirazi (S'10) was born in Tehran, Iran, 1983. He received the B.S. and M.S. degrees in electrical engineering from Isfahan University of Technology, Isfahan, Iran, in 2006 and 2009, respectively. He is currently pursuing the Ph.D. degree in Mechatronics at Simon Fraser University, Canada.

His research interests are intelligent transportation, control systems, system identification, and self-tuning control.

Ahmad B. Rad (M'99-SM'02) is a Professor in the School of Mechatronic Systems Engineering, Simon Fraser University, Canada. His current research interests include autonomous systems; Robotics; Intelligent control; and Applications of soft computing in modeling and control.